nature machine intelligence

ARTICLES

https://doi.org/10.1038/s42256-020-00276-w

Check for updates

A deep learning framework for drug repurposing via emulating clinical trials on real-world patient data

Ruoqi Liu[1], Lai Wei[2] and Ping Zhang[1,2,3] ✉

Drug repurposing is an effective strategy to identify new uses for existing drugs, providing the quickest possible transition from bench to bedside. Real-world data, such as electronic health records and insurance claims, provide information on large cohorts of users for many drugs. Here we present an efficient and easily customized framework for generating and testing multiple candidates for drug repurposing using a retrospective analysis of real-world data. Building upon well-established causal inference and deep learning methods, our framework emulates randomized clinical trials for drugs present in a large-scale medical claims database. We demonstrate our framework on a coronary artery disease cohort of millions of patients. We successfully identify drugs and drug combinations that substantially improve the coronary artery disease outcomes but haven't been indicated for treating coronary artery disease, paving the way for drug repurposing.

Drug repurposing (also known as, drug repositioning) is a strategy to accelerate the drug discovery process by identifying novel uses for existing approved drugs[1]. The primary advantage of drug repurposing over traditional drug development is that it starts from compounds with well-characterized pharmacology and safety profiles and can substantially reduce the risk of adverse effects and attrition in clinical phases[2].

While many successful repurposed drugs (for example, Viagra for erectile dysfunction) have been discovered serendipitously[3], computation-based repurposing methods have developed recently by leveraging structural features of compounds or proteins[4,5], genome-wide association study (GWAS)[6], transcriptional responses[7] and gene expression[8]. These methods focus primarily on using pre-clinical information. Unfortunately, the clinical therapeutic effects in humans are not always consistent with pre-clinical outcomes[9].

In healthcare, real-world data (RWD)[10] refers to longitudinal observational data derived from sources that are associated with outcomes in a heterogeneous patient population in real-world settings, such as patient surveys, electronic health records (EHRs), and claims and billing activities. Since RWD are direct observations from human bodies, they become a promising source for drug repurposing. A few researchers have already validated a small number of repurposing drug candidates on RWD[11,12]. However, there are some limitations with these approaches. First, most studies are complementary (that is, the original hypotheses usually come from other studies). Second, their studied number of repurposing candidates is limited and unable to proactively generate de novo repurposing drug candidates.

In this study, we follow protocols of randomized clinical trial (RCT) design[13], and computationally screen repurposing candidates for beneficial effect by explicitly emulating the corresponding clinical trials using RWD. Considering the inherent characteristics of RWD (that is, temporal sequence data and existing confounding variables[14]), we apply deep learning and causal inference methodologies to control the confounders in RWD, and systematically estimate the drug effects on various disease outcomes. Specifically, the estimated drug effects are obtained by long short-term memory (LSTM)[15] and inverse probability of treatment weighting (IPTW)[16], on MarketScan claims data[17].

As a test case, we apply the proposed drug repurposing framework to a coronary artery disease (CAD) cohort of millions of patients and emulate RCTs for multiple drug candidates, estimating their effects on CAD progression outcomes.

In general, our contribution is threefold:

- We develop a framework for high-throughput screening of on-market drugs by emulating, for each drug, an RCT that evaluates its beneficial effect. This allows repurposed drug candidates to be proactively generated from existing large-scale RWD.
- We present an innovative study design for the estimation of a drug's effect from longitudinal observational data. The CAD cohorts are automatically derived under our framework, which accelerates the process of computational drug repurposing.
- We propose a propensity score estimation model based on deep learning to correct for confounding and selection biases. Experimental comparisons to the logistic-regression-based propensity score estimation model show that our proposed deep learning model effectively estimates drug effects from RWD, paving the way for drug repurposing.
- We evaluate the therapeutic effect of drug combinations, drug-class-levelled candidates on disease outcomes and further explore potential repurposing opportunities with different model parameters. We also compare our framework with three existing pre-clinical drug repurposing methods, which gives a favourable outcome.

Overall framework

We develop a high-throughput, computational drug-repurposing pipeline (Fig. 1) that, given a disease cohort (for example, CAD

[1]Department of Computer Science and Engineering, The Ohio State University, Columbus, OH, USA. [2]Department of Biomedical Informatics, The Ohio State University, Columbus, OH, USA. [3]Translational Data Analytics Institute, The Ohio State University, Columbus, OH, USA. ✉e-mail: zhang.10631@osu.edu

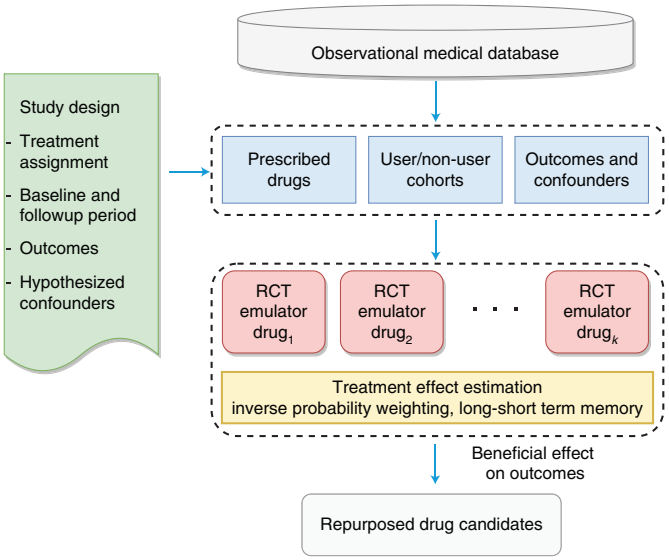

Fig. 1 | Flowchart of overall drug repurposing framework. First, a list of potential repurposing drug ingredients are extracted from the observational medical database given a disease cohort. Second, for each ingredient, the framework identifies the corresponding user and non-user sub-cohorts, and computes a large number of features for patients in both sub-cohorts. Third, the treatment effects are estimated via emulating an RCT for each ingredient to adjust confounding and biases.

patients), extracts a list of potential repurposing drug ingredients and, for each, identifies the corresponding user and non-user sub-cohorts. It then computes, for all patients in both sub-cohorts, a large number of features (confounding factors), as well as disease progression outcomes. The treatment effects are estimated after correcting for confounding and selection biases using the deep learning framework (Fig. 2). The framework is equipped with an attention mechanism that provides interpretability for the model. Drug ingredients with statistically significant beneficial effects will be considered as repurposed drug candidates and suggested as treatments for CAD. This algorithm shows an overview of the steps in estimating the effect of assigned treatment on the outcome from observational data:

Input: patient data: assigned treatment, outcomes, values for potential confounders

Output: repurposed drug candidates, and their estimated effect, unbalanced feature ratio and significance

1: Generate user and non-user sub-cohorts for the treatment
2: Compute balancing weights for all patients in both sub-cohorts via LSTM-based IPTW
3: Estimate the effect over multiple outcomes after correcting for the biases in the confounders (equation (1))
4: Compute the unbalanced feature ratio for the treatment after re-weighting using standardized difference (equation (2))
5: Estimate the significance of effect and compute adjusted p-values using bootstrapping
6: **if** estimated effect < 0 and adjusted p-value < 0.05 and unbalanced feature ratio $< 2\%$ **then**
7: **return** the estimated effect, unbalanced feature ratio and computed p-value
8: **end if**

Results

In this section we introduce the dataset we use for this study and then demonstrate the performance of our model in CAD drug repurposing experiments.

Dataset. We identified around 107.5 million distinct patients in the MarketScan Commercial Claims and Encounters (CCAE)[17] from 2012 to 2017, which contain individual-level, de-identified healthcare claims information from employers, health plans and hospitals. CCAE contains the largest number of patients and the most diverse population of the MarketScan data. The MartketScan table structure and data flow can be found in its user manual[18]. We extracted patient data from three source tables: Outpatient Drug (D), Inpatient Admission (I) and Outpatient Services (O). Then we compiled and formulated the raw data into five separate tables that can be easily prepossessed. The details of these tables and demo input data can be found in our Github repository at https://github.com/ruoqi-liu/DeepIPW.

MarketScan claims data are primarily used for evaluating health utilization and services. The overall distribution of patients during the recording period is shown in Extended Data Fig. 1a. We consider both inpatient and outpatient claims. CAD cohort criteria are defined using International Classification of Diseases (ICD) codes[19] (Supplementary Table 1). In total, there were 1,178,997 CAD patients. We refer to the first date when patients were diagnosed with CAD as their CAD initiation date. Extended Data Fig. 1b shows the patient distribution of time before/after CAD initiation date.

We identify three categories of study variable: demographic characteristics, diagnosis codes and prescription medication. Demographic characteristics in MarketScan CAD data include information on age and gender for each patient. Extended Data Fig. 1d shows the age and gender statistics distributions of our dataset. Because a majority of the data come from commercial claims, race and ethnicity information is incomplete and is not included in the analysis. Diagnosis codes in MarketScan CAD data are defined using the ICD codes for billing purposes. There are 57,089 ICD-9/10 codes considered in the dataset. Prescription medications in MarketScan CAD data also contain all prescription drug claims, which contain prescription drug name (generic and brand), national drug code (NDC) and the number of days of supply approved. By matching NDCs to observational medical outcomes partnership (OMOP) ingredient concept IDs[20], we get 1,353 unique drugs in the dataset for drug repositioning screening. For drugs with multiple ingredients, we consider each active ingredient separately in the mapping processes.

To evaluate the drug effect, we consulted domain experts to define a set of clinically relevant events linked to CAD as the disease outcomes (for example, heart failure onset and stroke onset). These definitions are based on ICD codes and can be found in Supplementary Tables 2 and 3. Since CAD is the major risk factor for both heart failure[21,22] and stroke[23,24], we hypothesize that an effective drug will lower the risks of CAD patients developing those diseases. Extended Data Fig. 1c demonstrates the time to develop outcomes from the CAD *initiation date*. The confounding variables affect both treatment assignment of patients and an outcome used in the trial. We consult domain experts to compile a list of hypothesized confounders for the CAD case study with respect to the study variables illustrate above: demographics, co-morbidities (diagnosis codes) and co-prescribed drugs.

Model performance. *Evaluation metrics.* Treatment effect estimation. In this study, we leverage average treatment effect (ATE) to examine the treatment effect at the population level, which is defined as

$$\mathrm{ATE} = \mathbb{E}(Y_1) - \mathbb{E}(Y_0) \quad (1)$$

where $\mathbb{E}(Y_1)$ and $\mathbb{E}(Y_0)$ are the expected potential treated and control outcomes of the whole population, respectively. The values of ATE are used to determine whether the given treatment can improve disease outcomes or not.

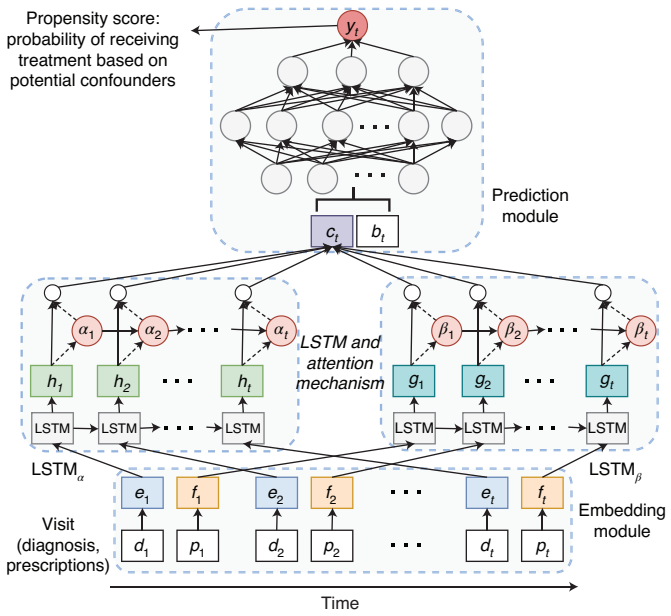

Fig. 2 | Illustration of the deep learning model for predicting treatment probability (or propensity score) that we used to correct confounding from time sequence data (including diagnoses d_t, prescriptions p_t and demographics b_t). It consists of three main components: an embedding module, a recurrent neural network (LSTM) and a prediction module.

Testing feature balance. We evaluate the performance of models by measuring features' balance between the weighted user and non-user sub-cohorts generated by the IPTW. Given patient weights from IPTW, we quantify the balance for each feature using its standardized mean difference (SMD), which is the difference in the variable means between the two treatment groups, divided by the combined standard deviation. To be exact, we use the following definition for standardized difference:

$$\mathrm{SMD} = \frac{|\mu_{\mathrm{user}} - \mu_{\mathrm{non-user}}|}{\sqrt{({s_{\mathrm{user}}}^2 + {s_{\mathrm{non-user}}}^2)/2}} \quad (2)$$

where μ_{user} and $\mu_{\mathrm{non\text{-}user}}$ are the mean in user cohort and non-user cohort; ${s_{\mathrm{user}}}^2$ and ${s_{\mathrm{non-user}}}^2$ are sample variance of variables in two sub-cohorts. For binary variables, the variance s^2 is calculated by $\mu(1-\mu)$. We consider a standardized difference greater than 0.1 as unbalanced[25] and compute the unbalanced feature ratio (that is, unbalanced/all features) before and after weighting to evaluate the performance of balancing. The user and non-user sub-cohorts are considered as balanced if their unbalanced feature ratio is below 2% after weighting.

Confidence intervals and significance of effect. We use bootstrapping[26] to calculate the confidence intervals of estimators of $\mathbb{E}(Y_1)$ and $\mathbb{E}(Y_0)$, and statistical significance of ATE. For each candidate ingredient, we repeatedly generate multiple different control drugs via random sampling with replacement, and the analysis is repeated in each bootstrap sample. The 95% confidence interval is then computed by using the standard normal approximation: ± 1.96 times the estimate of the standard error. The p-value of the effect estimator can be computed by the normal cumulative distribution function of estimators. We use adjusted p-value[27] as a statistically significant measurement. We consider a repurposing drug candidate as significant if its adjusted p-value is below 0.05.

Performance over repurposing drug candidates. We identified 55 qualified drugs following our study design (Methods). Then we estimated the treatment effect on various disease outcomes (that is, heart failure and stroke). The flowchart of data collection and study process can be found in Supplementary Fig. 2.

Among the qualified drugs obtained from the data, four of them are known CAD treatments: amlodipine, diltiazem, ticagrelor and rosuvastatin (drug label information is collected from SIDER[28] and DrugBank[29]). Our framework successfully retrieved three of these known drugs: amlodipine, diltiazem and rosuvastatin. We demonstrate the distribution of estimated ATE in Fig. 3. Here, we show the drug candidates with balanced user and non-user sub-cohorts after re-weighting and statistically significant estimates (adjusted p-value). All the drugs are ranked from left to right according to increasing estimated ATE values. Based on the definition of ATE (that is, the weighted average of observed outcomes from the user and non-user sub-cohorts), the drug ingredients with ATE values smaller than 0 are identified as improving disease outcomes, while the drug ingredients with ATE values larger than 0 are identified to worsen disease outcomes. For drugs with beneficial effects, we colour those with known CAD indications in red and those without in blue.

From the results, we observe that nine drugs yield a beneficial effect on disease outcomes among the sixteen selected significant drug candidates. Specifically, only three have been indicated for CAD according to their drug labels information. The remaining six drugs, which have not been indicated for treating CAD but can improve the disease outcomes, are considered as repurposed drug candidates. We find evidence to support these six drug candidates from related literature and web resources as follows: (1) metoprolol is one of the most commonly used beta-blockers for treating high blood pressure and chest pain. It shows beneficial effects in patients with heart failure associated with CAD[30]; (2) fenofibrate is mainly used to treat abnormal blood lipid levels and also appears to decrease the risk of CAD in patients with diabetes mellitus[31]; (3) hydrochlorothiazide, which is often used to treat high blood pressure and diabetes insipidus[32], also shows effectiveness in preventing CAD[33]; (4) pravastatin has also shown a beneficial effect on CAD[34]; (5) for simvastatin, results from RCTs show that it can reduce the occurrence of heart failure in patients with CAD[35]; (6) valsartan, a kind of angiotensin receptor blocker, results in improved coronary micro-vascular flow reserve, suggesting a direct benefit in hypertensive patients with stable CAD[36].

We further list the sub-cohort size, feature balancing and estimated ATE values for each drug candidate in Table 1. The results of all 55 drugs can be found in Supplementary Table 4. The first column lists the names corresponding to drugs in Fig. 3. The second and third columns denote the number of patients in user and non-user sub-cohorts, respectively. The next two columns denote the average number of unbalanced covariates before and after re-weighting. The unbalanced ratio column represents the ratio of unbalanced covariates to all covariates after re-weighting (that is, the number of unbalanced covariates divided by the total number of covariates). And the last two columns are the estimated ATE before and after re-weighting. We rank the drugs by increasing re-weighted ATE values. We see that our proposed method successfully corrects for most biases in the original data, which results in a decrease in the number of unbalanced covariates.

Attention visualization case studies. Having shown that our model successfully identified repurposed drug candidates for CAD treatment, we further demonstrate the interpretability of our framework achieves via attention mechanism. To exemplify this, we select two case drug candidates: diltiazem and fenofibrate. According to Table 1, diltiazem and fenofibrate both have beneficial effects on CAD disease outcomes. Diltiazem has already been used for treating CAD[37], while fenofibrate does not have CAD indication on its drug label.

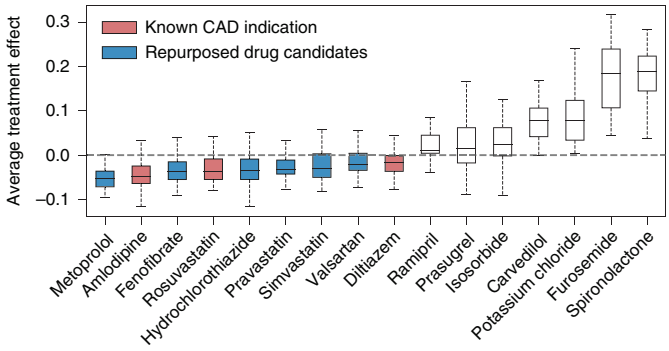

Fig. 3 | Distribution of estimated ATE of drugs on defined outcomes across the 50 bootstrap samples. All shown drugs satisfy two conditions: adjusted p-value ≤ 0.05 and post-weighting unbalanced ratio ≤ 2%. Within the boxplot, the central line denotes the median, and the bottom and the top edges denote the 25th (Q1) and 75th (Q3) and percentiles respectively. The whiskers extend to 1.5 times the interquartile range.

We want to identify the covariates that are greatly biased between the user and non-user cohorts in original data but balanced after re-weighting. The learned attention weights enable visualization of each covariate and its SMD values before/after balancing between the user and non-user cohorts. We select the top 20 well-balanced (that is, large deviations of SMD during balancing) covariates and plot the distribution of SMD values for two case drugs in Fig. 4. The original unweighted data are denoted as blue dots and LSTM-weighted data as orange dots. The covariates are ordered from bottom to top according to the increase of differences between SMD values of unweighted data and LSTM-weighted data. According to the figure, we see that for both drugs, the SMD values in the original data are greater than 0.1 (that is, the threshold of balancing), which indicates that the original observational data is highly biased and many confounding variables exist. The maximum SMD value is about 0.6 for diltiazem and 0.35 for fenofibrate. While the SMD values estimated in the LSTM-weighted data are smaller than 0.1, which means no major biases between the user and non-user cohorts in terms of selected covariates. The selected covariates include demographics (for example, age), co-prescribed drugs (metformin, metoprolol and so on) and co-morbidities (for example, acute myocardial infarction, cardiac dysrhythmias and so on). Correcting for these confounding variables gives a more accurate estimation of the treatment effect on the diseases.

Discussion

In this section, we demonstrate the model performance by comparing our framework with a logistic regression (LR)-based propensity score estimation method, and three existing pre-clinical drug repurposing methods. We also explore additional repurposing opportunities with drug class, synergistic drug combinations and various model parameters, further demonstrating the potential of our deep learning framework.

Comparison with an LR-based method. We also developed a base version of our model that uses LR for computing propensity score and treatment effect estimation. A recent study identifying drug repurposing candidates from observational data achieved a good performance on a case study of Parkinson's disease[38]. They estimated the propensity scores using LR. Thus, we conduct comparison experiments using the base model (LR-IPTW) and our model (LSTM-IPTW) on the two case drugs above and show the results for diltiazem in Extended Data Fig. 2 (the results for fenofibrate can be found in Supplementary Fig. 1).

As feature balancing is one of the most important evaluation metrics, we first plot the distribution of absolute SMD values computed by LSTM-IPTW and LR-IPTW (Extended Data Fig. 2a,d). In both LSTM- and LR-weighted data, many features exhibit large absolute SMD values (greater than 0.1) in the original data, while most features exhibit low absolute SMD (below 0.1) after re-weighting. Specifically, fewer features exhibit absolute SMD values above 0.1 thresholds after weighting by the LSTM model than weighting by the LR model. This indicates that the data is well balanced by LSTM-IPTW and the estimated ATE from LSTM-IPTW should be more accurate than LR-IPTW. Extended Data Fig. 2b shows the propensity distribution plot over user and non-user cohorts using LSTM-IPTW and LR-IPTW models. We observe that the propensity distribution of LSTM-IPTW is more smooth (that is, the propensities are normally distributed) than the distribution of LR-IPTW. Under the LR-IPTW model, many of the patients in non-user cohorts are predicted to have a propensity of 0. We also evaluated our models using conventional metrics. The receiver operating characteristic (ROC) curve is a standard metric widely used to estimate the performance of prediction models. The area under the ROC curve (AUC) characterizes the accuracy of the prediction results. Extended Data Fig. 2c,f shows the ROC curves for the LSTM-IPTW and LR-IPTW models. The 'propensity' curves in the figures are the standard ROC curves of the LSTM and the LR models. By comparing the AUC values of the two models, we see that the LSTM model yields more accurate prediction results than the LR model. With the accurate treatment predictions, the model would generate better weights for balancing and treatment effect estimates in the following tasks. Besides the standard ROC curve, we also show another two curves: the weighted propensity curve and expected curve, which are also leveraged for evaluating causal inference algorithms[39]. The weighted propensity curve is obtained by re-weighting the standard ROC curve using weights drawn from the propensity model (the same weights applied in covariate balancing and effect estimates). This curve should be very close to the curve that would arise by a random assignment (that is, with an AUC close to 0.5), which indicates our assumption that the weighting can emulate an RCT. From the plots, we find that LSTM-IPTW performs better than LR-IPTW in terms of being closer to 0.5. Compared with the standard propensity ROC curve, the 'expected' ROC curve duplicates the population and assigns weights to each individual based on the propensity. In this setting, each patient contributes their propensity to the true positives and (1 − propensity) to the false positives. The standard propensity ROC curve should be close to the expected propensity ROC. We observe that the propensity curve of LSTM-IPTW is much closer to its expected curve than LR-ITPW.

Additional experiments on drug class. We further consider the drug classes as repurposing candidates to extend the current framework, showing that our repurposing framework can also be applied to drug class level. We group the drugs into sub-classes according to ATC fourth-level (indicating chemical, therapeutic or pharmacological sub-group). Then we regard each drug sub-class as a repurposing candidate and emulate, for each candidate, an RCT to evaluate its treatment effect. The study design remains the same as that for individual drugs except that our studied repurposing candidates are drug classes (ATC fourth level). By applying the selection criteria and study design, we obtain 38 (out of 247) eligible drug classes.

We plot the distribution of estimated ATE values in Extended Data Fig. 3 (the mapping of ATC codes and drug class names is shown in Extended Data Fig. 4). Here, we only show the drug classes with the balanced user and non-user sub-cohorts after re-weighting and statistically significant estimates (adjusted p-value). The results of all 38 drug classes can be found in Supplementary Table 5.

Table 1 | The estimated treatment effects for CAD over balanced and statistically significant drug ingredients

Drug name	Users	Non-users	Unbalanced covariates (pre)	Unbalanced covariates (post)	Covariates	Unbalanced ratio (post)	ATE (pre)	ATE (post)
Metoprolol	**9,730**	**29,190**	**38.308**	**23.231**	**1,270**	**1.8**	**−0.023**	**−0.043**
Fenofibrate	**1,352**	**4,056**	**39.340**	**13.200**	**1,038**	**1.3**	**−0.051**	**−0.038**
Rosuvastatin	2,420	7,260	24.020	9.620	1,097	0.9	−0.063	−0.030
Hydrochlorothiazide	**2,001**	**6,003**	**32.500**	**15.320**	**1,076**	**1.4**	**−0.055**	**−0.029**
Amlodipine	4,613	13,839	21.340	8.300	1,180	0.7	−0.050	−0.026
Pravastatin	**2,007**	**6,021**	**11.260**	**9.640**	**1,085**	**0.9**	**−0.016**	**−0.022**
Simvastatin	**1,605**	**4,815**	**10.060**	**13.240**	**1,044**	**1.3**	**−0.032**	**−0.020**
Valsartan	**1,316**	**3,948**	**24.940**	**13.740**	**1,026**	**1.3**	**0.010**	**−0.015**
Diltiazem	1,044	3,132	28.360	13.080	1,007	1.3	−0.010	−0.013
Isosorbide	1,482	4,446	33.320	9.560	1,039	0.9	0.045	0.034
Prasugrel	1,316	3,948	41.500	18.340	1,019	1.8	−0.043	0.036
Ramipril	887	2,661	25.340	14.840	973	1.5	0.020	0.043
Potassium chloride	1,110	3,330	43.460	20.240	1,016	2.0	0.169	0.090
Carvedilol	3,959	11,877	38.280	8.140	1,154	0.7	0.198	0.124
Furosemide	1,545	4,635	50.880	17.080	1,064	1.6	0.301	0.179
Spironolactone	1,292	3,876	70.620	12.920	1,034	1.3	0.393	0.190

Bold denotes ingredients without a known CAD indication (repurposed drug candidates). The drugs are ranked by the estimated ATE values. Pre and post refer to re-weighting.

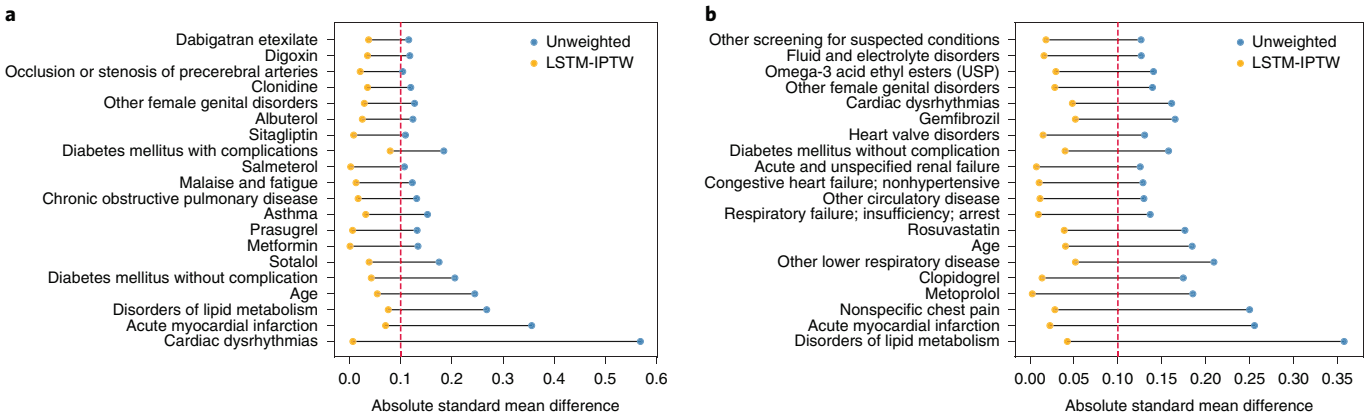

Fig. 4 | The SMD values of the top 20 well-balanced covariates. a, Diltiazem results. **b**, Fenofibrate results. The dashed red lines indicate the threshold of balancing.

All the drug classes are ranked left to right according to the increasing order of estimated ATE values. From the results, we observe that 12 drug classes yield a beneficial effect on disease outcomes among 16 selected significant drug classes.

We also compare the results of drug classes to previous results based on drug ingredients. We observe that most extracted drug classes are consistent with the extracted drug classes in Table 1, while some of them are not. For example, three extracted significant drug ingredients: rosuvastatin, pravastatin and simvastatin, belong to drug class HMG CoA reductase inhibitors (ATC code: C10AA), whereas HMG CoA reductase inhibitors is not a significant drug class. Also, some drug classes (for example, 'other antidepressants' and "selective serotonin reuptake inhibitors") show a beneficial effect with statistical significance in Extended Data Fig. 4, but the drugs that belong to them are not significant nor beneficial to the disease in Table 1.

Drug class offers additional information for drug discovery or drug repurposing tasks. Considering the drug class helps to uncover potential repurposing drug candidates from the drug classes. In future work, we will consider the drug class for drug discovery/repurposing with a more comprehensive analysis.

Additional experiments on drug combinations. We also evaluate the effect of drug combinations on CAD disease progression. Similar to the experimental setting of individual drugs, we select drug combinations that satisfy the previous cohort definition and criteria (that is, the number of minimum patients in a cohort is no less than 500, window thresholds, persistent prescription and so on). After applying the cohort selection, we obtain seven drug combinations: (1) metoprolol and clopidogrel; (2) metoprolol and atorvastatin; (3) lisinopril and atorvastatin; (4) lisinopril and clopidogrel; (5) metoprolol and lisinopril; (6) clopidogrel and atorvastatin; (7) carvedilol and atorvastatin.

We demonstrate the significant drug combinations in Extended Data Fig. 5 (the full list of drug combinations can be found in Supplementary Table 6). As shown in some drugs are not significant

when evaluating their effectiveness at the individual level, while they are significant when combined with others. For example, lisinopril and atorvastatin are not statistically significant as individual treatments, but their drug combination is significant and has a beneficial effect on the outcomes. These results illustrate that considering the synergies of drug combinations provides further interesting findings of potential repurposing.

Comparison with pre-clinical-based methods. We compare our method with three existing pre-clinical drug repurposing methods[40–42] and conduct experiments using CAD as a case study. From the literature[43,44], we know that drug chemical structures, protein targets and chemical–protein interactome (CPI) docking are very important for computational pre-clinical drug repurposing methods. We followed the experimental settings of Gottlieb et al.[45] to predict drugs for CAD. Specifically, we built an 881-dimensional binary vector for chemical structures following Zhang et al.[40] and Liang et al.[41]. We built a 1,210-dimensional binary vector for protein targets following Zhang et al.[40] and Liang et al.[41]. And we built a 600-dimensional continuous vector for CPI docking scores following Luo et al.[42] and Luo et al.[4].

For the performance evaluation, we used precision at K (precision@K) as our main evaluation metric to see how many drugs can be validated among the top-ranked candidates. We chose precision@K because given a limited budget, pharmaceutical companies can only evaluate the top-ranked drug candidates instead of all existing on-market drugs. As shown in Extended Data Fig. 6, our method performs better than the other three pre-clinical methods that use CPI docking, drug chemical structures and drug targets as features, respectively. Compared with pre-clinical methods, our method demonstrates two further advantages: (1) fewer translational problems[9]: we use observational data and emulate the process of RCTs while they only leverage pre-clinical information; (2) it's more robust: we have strict covariate balancing testing and significance testing that guarantee our results are robust and convincing.

Influence of the model parameters to the results. We also study the influence of one of our model parameters: adjusted *p*-value to the results. We slightly relax the threshold for adjusted *p*-value from 0.05 to 0.15 (ref. [46]) and keep the post-weighting unbalanced ratio the same as before. Extended Data Fig. 7 shows the additional repurposing candidates retrieved under this parameter setting (adjusted *p*-value is less than 0.15 and the post-weighting unbalanced ratio is less than 0.02). As shown in Extended Data Fig. 7, four more drugs are retrieved by our framework. Specifically, (1) metformin, which is the first-line medication for the treatment of type 2 diabetes, and has also been tested for treating CAD in clinical trials[47]; (2) escitalopram, used to treat major depressive disorder or generalized anxiety disorder[48], and some studies have started to explore the drug repurposing opportunity for CAD[49]; (3) atorvastatin has already been studied in a clinical trial for evaluating its therapeutic effect on CAD[50]; and (4) losartan has also been included in clinical trials[51].

By relaxing the adjusted *p*-value threshold, we have more drug candidates (for example, metformin and escitalopram) with diverse indications. Our goal is to develop a general computational framework for drug repurposing. For people who want to use our framework, they can easily adjust these parameters according to their preference.

This study can be extended in multiple directions in the future. For this study, we used hypothesized confounders including demographics, co-morbidities and co-prescribed drugs. Some other potential confounders such as time elapsed from the first disease diagnosis to index date and outcome value calculated over the baseline period could be considered to build the model in the future work.

In summary, we demonstrate that the proposed computational drug repurposing framework can successfully identify drug candidates that have a beneficial effect on disease outcomes but aren't yet indicated for CAD patients. The proposed LSTM-IPTW model performs better at correcting biases and estimating treatment effects than LR-IPTW, and retaining interpretability for recognizing important confounding. We also evaluate the therapeutic effect of drug combinations, drug-class-level candidates on disease outcomes and further explore the potential repurposing opportunity with different model parameters. Besides, we compare our framework with three existing pre-clinical drug repurposing methods and our framework outperforms others.

Methods

In this section, we introduce the study design, which includes definitions of cohorts and study variables. Then we illustrate our deep learning model in detail with three main components.

Study design. Our framework identifies drug repurposing candidates using MarketScan CAD data to emulate a bulk of corresponding RCTs. Below, we describe the design of the emulated trials and the key components of our framework for CAD drug repurposing.

User and non-user cohorts. Given the drug tested in the trial, a patient is assigned to the user cohort if the following inclusion criteria are satisfied: (1) the patient has been persistently prescribed the drug (for example, the interval between two prescriptions is less than 30 days); (2) the patient is eligible for trial at the time of the first prsquocription for the drug (in the CAD study, this condition is that the first prescription is after the CAD initiation date); (3) the patient had at least one year's (365 days) history in the database prior to the first prescription of the drug.

Estimating the effect of a drug requires comparing the user cohort to a control group assigned with alternative drugs. Once the alternative drugs are determined, the non-user cohort is defined by the same inclusion criteria described above—but with respect to the alternative drugs. To avoid overlap between the user and non-user cohorts, the framework further excludes from the non-user cohort any patient prescribed with the trial's drug. In our study design, alternative drugs are selected randomly from the prescribed ingredients, excluding the trial drug itself. Such a control group directly compares the trial's drug to drugs of the same therapeutic indication, reducing confounding by indication. We use the term "index date" to refer to the date of the first prescription of the assigned drug, that is, the first time the trial's drug (respectively, the alternative drug) was prescribed for patients in the user (respectively, non-user) cohort.

Baseline and follow-up periods. We refer to the time period prior to the index date for which we have information on the patient as the baseline period. We use the baseline period for characterizing the patients prior to the beginning of the treatment with the assigned drug. The follow-up period starts at the index date, that is, at the beginning of the treatment with the trial's drug in the user cohort, and the control drug in the non-user cohort. The effect of the drug is evaluated during the follow-up period. In the CAD study, the baseline period is at least 365 days, and the follow-up period is 2 years (730 days). Extended Data Fig. 8 demonstrates the definition of user and non-user cohorts.

Outcomes and hypothesized confounders. The effect of the drug during the follow-up period is defined with respect to various disease outcomes. In this CAD drug repurposing case study, we consulted domain experts to define a set of clinically relevant events linked with CAD as the outcome, for example, heart failure onset (Supplemental Table 2) and stroke onset (Supplemental Table 3). The treatment effect is estimated on these outcomes during the follow-up period (that is, 730 days after the index date). The patient is considered to have the disease outcome if either of them happens in the follow-up period.

Confounders are variables affecting both treatment assignment of patients and an outcome used in the trial, thus creating a 'backdoor path' that may hinder the true effect of the drug on the outcome. We consult domain experts to compile a list of hypothesized confounders for the CAD study, including demographics (for example, age at the index date and sex), co-morbidities (for example, indicator per each ICD-9/10 diagnosis class) and co-prescribed drugs. Since confounders affect treatment assignment, they are computed on the baseline period.

Repurposing drug ingredients. We regard a drug as a repurposing candidate if it satisfies the following conditions: (1) contains an active ingredient (that is, the ingredient directly involved in achieving the mediation objectives); and (2) is persistently prescribed to a large enough number of patients in the disease cohort. Specifically, an ingredient is considered as being used by a patient only if it was prescribed on two or more distinct dates, as least one month apart. And a minimum of 500 patients prescribed a certain ingredient was required. For each repurposing candidate, we can compute the user and non-user cohorts according

to the above definition of cohorts. After obtaining the corresponding user and non-user cohorts, we can extract outcomes and hypothesized confounders for each individual patient from the database. Every patient in their sub-cohort is represented by a sequence of events, with each event providing the patient information (that is, co-morbidities, co-prescribed drugs and so on) that corresponds to each visit. The available data within these visits during the baseline period, combined with demographic characteristics (that is, age and gender collected at CAD initiation date) are used as inputs to the model.

Model. *Estimation of ATE.* Our proposed framework evaluates the effect of a certain drug (that is, a trial's drug) on a clinical outcome with respect to alternative treatments. Let $\alpha=1$ denote the treatment corresponding to the trial's drug, and $\alpha=0$ denote the alternative treatments. We define the ATE of a drug on the potential outcome Y as $\text{ATE} = \mathbb{E}(Y_1) - \mathbb{E}(Y_0)$, with $\mathbb{E}(Y_\alpha)$ denoting the potential expected prevalence of patients who would have experienced an outcome event during a complete follow-up period if all patients in the trial had been assigned with treatment α. The potential outcomes are referred to as counterfactual as only one of these is observed for any given individual. By running RCTs, we can measure the outcomes within user and non-user groups into which individuals are randomly assigned: $\mathbb{E}(Y_1)$ can be directly estimated as $\mathbb{E}(Y|\alpha = 1)$ and $\mathbb{E}(Y_0)$ as $\mathbb{E}(Y|\alpha = 0)$. However, in observational data (for example, our MarketScan CAD data), treatment assignment is usually far from random, which may depend on confounders (affecting both treatment assignment and outcome). We need to assign weights to the individuals in each group to avoid the influence of confounders.

In order to control the influence of confounders, we apply IPTW to create a pseudo-population from the original one by assigning a weight w_i^α to an individual i with treatment α. The weight is defined as the inverse of the conditional probability (or propensity score) that an individual is treated with α given the confounding values. One common issue with IPTW is that individuals with a propensity score very close to 0 will end up with an extremely high weight, potentially making the weighted estimator unstable. We address this problem by adopting an alternative weighting function called standardized IPTW[25], which uses the marginal probability of treatment instead of 1 in the weight numerator.

Logistic regression is the most popular method in statistics for estimating the propensity score[52]. In longitudinal observational data, those observational covariates are not a set of static feature vectors (one for each patient), but irregularly sampled time series (recording diagnoses, medications and so on at each timestamp). Thus, logistic regression is not ideal for effectively modelling longitudinal observational data.

Model for propensity score weighting. The schematic view of our model is shown in Fig. 2, which consists of three main components: an embedding module, a recurrent neural network and a prediction module. Briefly, the model estimates the propensity score by first transforming the input features using an embedding layer. These embedded features are then fed into LSTM, the output of which at every time point is aggregated through an attention layer for automatically focusing on important time points. The aggregated features are fed into a prediction module that provides the probability of receiving treatment. Each of these is discussed below in detail.

Embedding module. The embedding module is to convert the initial high-dimensional and sparse input features into a lower-dimensional and continuous data representation, which is beneficial to the following prediction task. As shown in Fig. 2, the input features consist of three components: diagnosis, prescription and demographic information (age and gender). The diagnosis codes for each patient at each timestamp can be denoted as $\{\mathbf{d}_1, \mathbf{d}_2, \ldots, \mathbf{d}_t\}$, and prescription can be denoted as $\{\mathbf{p}_1, \mathbf{p}_2, \ldots, \mathbf{p}_t\}$. Here, $\mathbf{d}_t$ and $\mathbf{p}_t$ are both one dimensional binary vectors with the size of diagnosis code dictionary (r) and prescription code dictionary (s), respectively. For each element in the vector, the value in the j-th column indicates that code j is documented in the t-th visit. We use two linear embedding modules to represent diagnosis and prescription respectively. That is, we define $\mathbf{e}_t = \mathbf{W}^d_{\text{emb}}\mathbf{d}_t$, $\mathbf{f}_t = \mathbf{W}^p_{\text{emb}}\mathbf{p}_t$, where $\mathbf{e}_t \in \mathbb{R}^m$ denotes the embedding of the input vector $\mathbf{d}_t \in \mathbb{R}^r$, m is the size of the diagnosis embedding dimension, and $\mathbf{W}^d_{\text{emb}} \in \mathbb{R}^{m\times r}$ is the embedding matrix. $\mathbf{f}_t \in \mathbb{R}^n$ denotes the embedding of the input vector $\mathbf{p}_t \in \mathbb{R}^s$, n is the size of the diagnosis embedding dimension, and $\mathbf{W}^p_{\text{emb}} \in \mathbb{R}^{n\times s}$ is the embedding matrix. The age is normalized into a range of [0, 1] using min–max normalization and the gender is represented as a binary vector. Having the embedded vectors of patients, we input them to LSTM.

Recurrent neural network and attention mechanism. LSTM[15], which is a kind of recurrent neural network equipped with memory cells, can better model the temporality of observational data. A common LSTM unit contains a cell, an input gate, an output gate and a forget gate. The cell can remember values over irregular time intervals and the three gates moderate the flow of information into and out of the cell. The inputs to the LSTM are embedded confounding vectors from the embedding module and the output of which is the patient's latent health status at the time of visit. We use two LSTMs, LSTM_α and LSTM_β to separately model diagnosis and prescription codes of patients.

$$\begin{aligned}\mathbf{h}_1, \mathbf{h}_2, ..., \mathbf{h}_t &= \text{LSTM}_\alpha(\mathbf{e}_1, \mathbf{e}_2, ..., \mathbf{e}_t)\\ \mathbf{g}_1, \mathbf{g}_2, ..., \mathbf{g}_t &= \text{LSTM}_\beta(\mathbf{f}_1, \mathbf{f}_2, ..., \mathbf{f}_t)\end{aligned} \tag{3}$$

where $\mathbf{h}_t \in \mathbb{R}^u$, $\mathbf{g}_t \in \mathbb{R}^v$ are hidden state vectors at t-th visit, and u and v denote the size of hidden layer of LSTM_α and LSTM_β. Then those patient hidden states are aggregated through two separate attention layers for automatically focusing on important visits.

$$\begin{aligned}\alpha_i &= \text{Softmax}\,(\mathbf{W}_\alpha^\top \mathbf{h}_i + \mathbf{b}_\alpha), \quad \text{for } i = 1, 2..., t\\ \mathbf{c}_\alpha &= \textstyle\sum_{i=1}^t \alpha_i \mathbf{h}_i\\ \beta_i &= \text{Softmax}\,(\mathbf{W}_\beta^\top \mathbf{g}_i + \mathbf{b}_\beta), \quad \text{for } i = 1, 2..., t\\ \mathbf{c}_\beta &= \textstyle\sum_{i=1}^t \beta i \mathbf{g}_i\end{aligned} \tag{4}$$

where $\mathbf{W}_\alpha \in \mathbb{R}^u$, $\mathbf{b}_\alpha \in \mathbb{R}^u$, $\mathbf{W}_\beta \in \mathbb{R}^v$ and $\mathbf{b}_\beta \in \mathbb{R}^v$ are the parameters to learn. Using the generated attention weights for diagnosis and prescription, we obtain the aggregated vectors $\mathbf{c}_\alpha \in \mathbb{R}^u$ and $\mathbf{c}_\beta \in \mathbb{R}^v$ as defined in equation (4). Then we combine $\mathbf{c}_\alpha$, $\mathbf{c}_\beta$ with vectorized age and gender to predict the probability of receiving a treatment (propensity score).

Prediction module. The aggregated patient states from attention layer $\mathbf{c}_\alpha$, $\mathbf{c}_\beta$, combined with the demographic features c_{demo}, are passed through a fully connected neural network to predict the probability of receiving a treatment as follows,

$$\hat{y} = \text{Sigmoid}\,(\mathbf{W}^\top \mathbf{c}_t + b) \tag{5}$$

where $\mathbf{c}_t = \text{ReLu}(\mathbf{W}_c[\mathbf{c}_\alpha, \mathbf{c}_\beta, c_{\text{demo}}] + \mathbf{b}_c)$, $\mathbf{W}_c \in \mathbb{R}^{k\times(u+v+2)}$, $\mathbf{b}_c \in \mathbb{R}^k$, $\mathbf{W} \in \mathbb{R}^k$, $b \in \mathbb{R}$ are the model parameters. We use cross-entropy to calculate the prediction loss as follows,

$$\mathcal{L} = -\frac{1}{N}\sum_{i=1}^N (y_i \log \hat{y}_i + (1 - y_i)\log(1 - \hat{y}_i)) \tag{6}$$

where y_i is the ground truth of observed treatment for patient i.

Experiment settings. The model is implemented and trained with Python 3.6 and PyTorch 1.4 (https://pytorch.org/), on a high-performance computing cluster with four NVIDIA TITAN RTX 6000 GPUs. For each drug candidate, we train a model using the adaptive moment estimation (Adam) algorithm with a batch size of 50 subjects and a learning rate of 0.001. We run each model for 50 iterations for computing p-values and confidence intervals. We randomly split the input data into training, validation and test sets with a ratio of 70:10:20. The information from a given patient is only present in one set. The training set is to train the proposed models. The validation set is used to improve the models and select the best model hyperparameters.

Data availability

The data we use is MarketScan Commercial Claims and Encounters (CCAE, more than 100 million patients, from 2012 to 2017) The details of source data structure and prepossessed input data demo are available at the Github repository https://github.com/ruoqi-liu/DeepIPW. Access to the MarketScan data analysed in this manuscript is provided by the Ohio State University. The dataset is available from IBM at https://www.ibm.com/products/marketscan-research-databases.

Code availability

The source code for this paper can be downloaded from the Github repository at https://github.com/ruoqi-liu/DeepIPWor the Zenodo repository at https://doi.org/10.5281/zenodo.4079391.

Received: 27 February 2020; Accepted: 16 November 2020;
Published online: 04 January 2021

References

1. Langedijk, J., Mantel-Teeuwisse, A. K., Slijkerman, D. S. & Schutjens, M.-H. D. Drug repositioning and repurposing: terminology and definitions in literature. *Drug Discov. Today* **20**, 1027–1034 (2015).
2. Ashburn, T. T. & Thor, K. B. Drug repositioning: identifying and developing new uses for existing drugs. *Nat. Rev. Drug Discov.* **3**, 673–683 (2004).
3. Pushpakom, S. et al. Drug repurposing: progress, challenges and recommendations. *Nat. Rev. Drug Discov.* **18**, 41–58 (2019).
4. Luo, H. et al. DPDR-CPI, a server that predicts drug positioning and drug repositioning via chemical-protein interactome. *Sci. Rep.* **6**, 35996 (2016).
5. Dakshanamurthy, S. et al. Predicting new indications for approved drugs using a proteochemometric method. *J. Med. Chem.* **55**, 6832–6848 (2012).
6. Sanseau, P. et al. Use of genome-wide association studies for drug repositioning. *Nat. Biotechnol.* **30**, 317–320 (2012).
7. Iorio, F. et al. Discovery of drug mode of action and drug repositioning from transcriptional responses. *Proc. Natl Acad. Sci USA* **107**, 14621–14626 (2010).

8. Sirota, M. et al. Discovery and preclinical validation of drug indications using compendia of public gene expression data. *Sci. Transl. Med.* **3**, 96ra77 (2011).
9. Buchan, N. S. et al. The role of translational bioinformatics in drug discovery. *Drug Discov. Today* **16**, 426–434 (2011).
10. Sherman, R. E. et al. Real-world evidence—what is it and what can it tell us. *N. Engl. J. Med.* **375**, 2293–2297 (2016).
11. Cheng, F. et al. Network-based approach to prediction and population-based validation of in silico drug repurposing. *Nat. Commun.* **9**, 2691 (2018).
12. Xu, H. et al. Validating drug repurposing signals using electronic health records: a case study of metformin associated with reduced cancer mortality. *J. Am. Med. Inform. Assoc.* **22**, 179–191 (2014).
13. Hernán, M. A. & Robins, J. M. Using big data to emulate a target trial when a randomized trial is not available. *Am. J. Epidemiol.* **183**, 758–764 (2016).
14. D'Agostino, R. B. Estimating treatment effects using observational data. *JAMA* **297**, 314–316 (2007).
15. Hochreiter, S. & Schmidhuber, J. Long short-term memory. *Neural Comput.* **9**, 1735–1780 (1997).
16. Hirano, K., Imbens, G. W. & Ridder, G. Efficient estimation of average treatment effects using the estimated propensity score. *Econometrica* **71**, 1161–1189 (2003).
17. MarketScan Research Databases. *IBM* https://www.ibm.com/products/marketscan-research-databases (2020).
18. *Commercial Claims and Encounters: Medicare Supplemental* https://theclearcenter.org/wp-content/uploads/2020/01/IBM-MarketScan-User-Guide.pdf (Truven Health Analytics, 2016).
19. Classification of diseases, functioning, and disability. *Centers for Disease Control and Prevention* https://www.cdc.gov/nchs/icd/index.htm (2019).
20. The Observational Health Data Sciences and Informatics (OHDSI). https://ohdsi.org/ (2019).
21. Causes of heart failure. *American Heart Association* https://www.heart.org/en/health-topics/heart-failure/causes-and-risks-for-heart-failure/causes-of-heart-failure (2017).
22. Gheorghiade, M. & Bonow, R. O. Chronic heart failure in the united states: a manifestation of coronary artery disease. *Circulation* **97**, 282–289 (1998).
23. Conditions that increase risk for stroke. *Centers for Disease Control and Prevention* https://www.cdc.gov/stroke/conditions.htm (2018).
24. Coronary artery disease. *Heart and Stroke Foundation of Canada* https://www.heartandstroke.ca/heart/conditions/coronary-artery-disease (2019).
25. Austin, P. C. An introduction to propensity score methods for reducing the effects of confounding in observational studies. *Multivariate Behav. Res.* **46**, 399–424 (2011).
26. Efron, B. & Tibshirani, R. Bootstrap methods for standard errors, confidence intervals, and other measures of statistical accuracy. *Stat. Sci.* **1**, 54–75 (1986).
27. Benjamini, Y. & Hochberg, Y. Controlling the false discovery rate: a practical and powerful approach to multiple testing. *J. R. Stat. Soc. B* **57**, 289–300 (1995).
28. Kuhn, M., Campillos, M., Letunic, L. J. & Bork, P. A side effect resource to capture phenotypic effects of drugs. *Mol. Syst. Biol.* **6**, 343 (2010).
29. Wishart, D. S. et al. Drugbank 5.0: a major update to the drugbank database for 2018. *Nucleic Acids Res.* **46**, D1074–D1082 (2018).
30. Fisher, M. L. et al. Beneficial effects of metoprolol in heart failure associated with coronary artery disease: a randomized trial. *J. Am. Coll. Cardiol.* **23**, 943–950 (1994).
31. Wong, T. Y., Simó, R. & Mitchell, P. Fenofibrate – a potential systemic treatment for diabetic retinopathy?. *Am. J. Ophthalmol.* **154**, 6–12 (2012).
32. Hydrochlorothiazide. *drugs.com* https://www.drugs.com/monograph/hydrochlorothiazide.html (2019).
33. Pepine, C. J. et al. A calcium antagonist vs a non–calcium antagonist hypertension treatment strategy for patients with coronary artery disease: the international verapamil-trandolapril study (invest): a randomized controlled trial. *JAMA* **290**, 2805–2816 (2003).
34. Jukema, J. W. et al. Effects of lipid lowering by pravastatin on progression and regression of coronary artery disease in symptomatic men with normal to moderately elevated serum cholesterol levels: the regression growth evaluation statin study (regress). *Circulation* **91**, 2528–2540 (1995).
35. Kjekshus, J., Pedersen, T. R., Olsson, A. G., Færgeman, O. & Pyörälä, K. The effects of simvastatin on the incidence of heart failure in patients with coronary heart disease. *J. Card. Fail.* **3**, 249–254 (1997).
36. Higuchi, T., Abletshauser, C., Nekolla, S. G., Schwaiger, M. & Bengel, F. M. Effect of the angiotensin receptor blocker valsartan on coronary microvascular flow reserve in moderately hypertensive patients with stable coronary artery disease. *Microcirculation* **14**, 805–812 (2007).
37. Diltiazem. *SIDER* http://sideeffects.embl.de/drugs/3075/ (2019).
38. Ozery-Flato, M., Goldschmidt, Y., Shaham, O., Ravid, S. & Yanover, C. Framework for identifying drug repurposing candidates from observational healthcare data. Preprint at *medRxiv* https://doi.org/10.1101/2020.01.28.20018366 (2020).
39. Shimoni, Y. et al. An evaluation toolkit to guide model selection and cohort definition in causal inference. Preprint at https://arxiv.org/abs/1906.00442 (2019).
40. Zhang, P., Wang, F., Hu, J. & Sorrentino, R. Exploring the relationship between drug side-effects and therapeutic indications. In *AMIA Annual Symposium Proceedings 2013* 1568–1577 (American Medical Informatics Association, 2013).
41. Liang, X. et al. LRSSL: predict and interpret drug–disease associations based on data integration using sparse subspace learning. *Bioinformatics* **33**, 1187–1196 (2017).
42. Luo, H. et al. DRAR-CPI: a server for identifying drug repositioning potential and adverse drug reactions via the chemical–protein interactome. *Nucleic Acids Res.* **39**, W492–W498 (2011).
43. Dudley, J. T., Deshpande, T. & Butte, A. J. Exploiting drug–disease relationships for computational drug repositioning. *Brief. Bioinform.* **12**, 303–311 (2011).
44. Jarada, T. N., Rokne, J. G. & Alhajj, R. A review of computational drug repositioning: strategies, approaches, opportunities, challenges, and directions. *J. Cheminf.* **12**, 46 (2020).
45. Gottlieb, A., Stein, G. Y., Ruppin, E. & Sharan, R. PREDICT: a method for inferring novel drug indications with application to personalized medicine. *Mol. Syst. Biol.* **7**, 496 (2011).
46. Rubinstein, L. V. et al. Design issues of randomized phase II trials and a proposal for phase ii screening trials. *J. Clin. Oncol.* **23**, 7199–7206 (2005).
47. Metformin to reduce heart failure after myocardial infarction (gips-iii). *clinicaltrials.gov* https://clinicaltrials.gov/ct2/show/study/NCT01217307?term=metformin&cond=Coronary+Artery+Disease&phase=12&draw=2&rank=2 (2018).
48. Escitalopram oxalate. *drugs.com* https://www.drugs.com/monograph/escitalopram-oxalate.html (2020).
49. Responses of myocardial ischemia to escitalopram treatment (remit). *clinicaltrials.gov* https://clinicaltrials.gov/ct2/show/NCT00574847?term=escitalopram&cond=Coronary+Artery+Disease&draw=2&rank=1 (2015).
50. Effect of atorvastatin on fractional flow reserve in coronary artery disease (forte). *clinicaltrials.gov* https://clinicaltrials.gov/ct2/show/NCT01946815?term=atorvastatin&cond=Coronary+Artery+Disease&phase=12&draw=2&rank=1 (2018).
51. Dahlöf, B. et al. Cardiovascular morbidity and mortality in the losartan intervention for endpoint reduction in hypertension study (life): a randomised trial against atenolol. *Lancet* **359**, 995–1003 (2002).
52. D'Agostino, R. B. Jr Propensity score methods for bias reduction in the comparison of a treatment to a non-randomized control group. *Stat. Med.* **17**, 2265–2281 (1998).

Acknowledgements

This work was funded in part by the National Center for Advancing Translational Research of the National Institutes of Health under award number CTSA Grant UL1TR002733. The content is solely the responsibility of the authors and does not necessarily represent the official views of the National Institutes of Health.

Author contributions

P.Z. conceived the project. R.L. and P.Z. developed the method. R.L. conducted the experiments. R.L., L.W. and P.Z. analysed the results. R.L., L.W. and P.Z. wrote the manuscript. All authors read and approved the final manuscript.

Competing interests

The authors declare no competing interests.

Additional information

Extended data is available for this paper at https://doi.org/10.1038/s42256-020-00276-w.

Supplementary information is available for this paper at https://doi.org/10.1038/s42256-020-00276-w.

Correspondence and requests for materials should be addressed to P.Z.

Peer review information *Nature Machine Intelligence* thanks Daniel Merk and the other, anonymous, reviewer(s) for their contribution to the peer review of this work.

Reprints and permissions information is available at www.nature.com/reprints.

Publisher's note Springer Nature remains neutral with regard to jurisdictional claims in published maps and institutional affiliations.

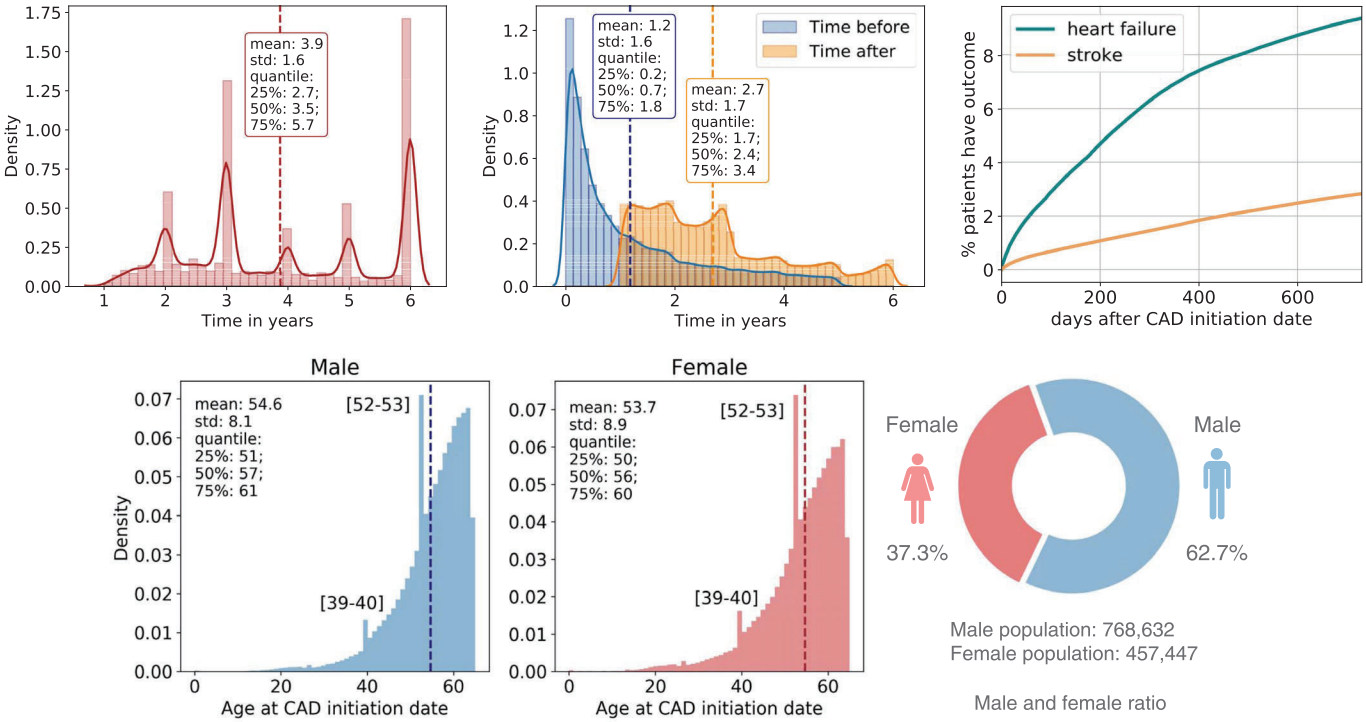

Extended Data Fig. 1 | CAD cohorts characteristics. a, The patients' distribution of total time in the database. **b**, The patient's distribution of time before/after CAD *initiation date*. **c**, The growth of the number of patients developing outcomes after CAD *initiation date*. **d**, The gender distribution with age at CAD *initiation date*.

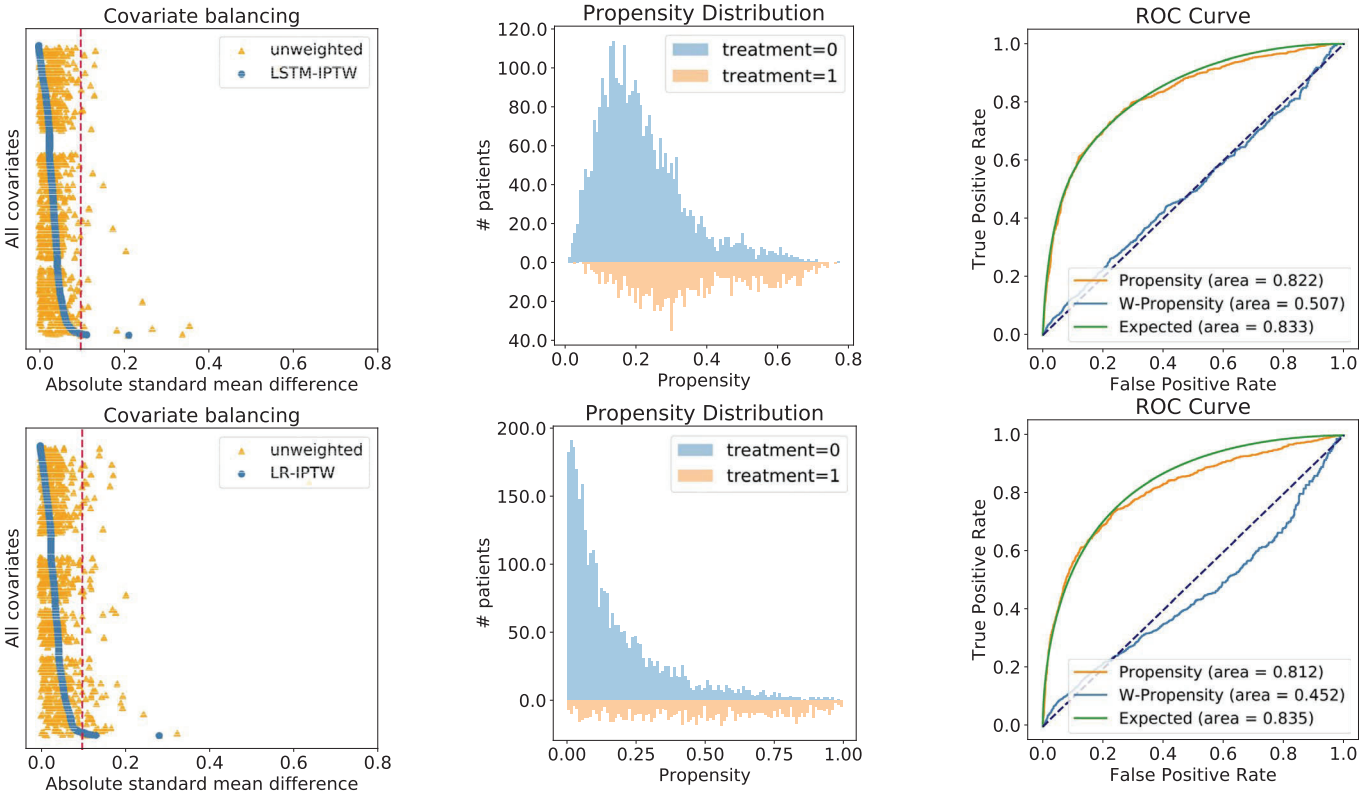

Extended Data Fig. 2 | Performance comparison of LSTM-IPTW and LR-IPTW using drug candidate: diltiazem (*with* known CAD indication). The three figures on the top are results obtained from LSTM-IPTW, while the figures on the bottom are from LR-IPTW. **a**, and (**d**) The absolute SMD of each covariate in the original data (orange triangles) and in the weighted data (blue circles). **b**, and (**e**) The distribution of estimated propensity scores over user (orange area) and non-user (blue area) cohorts. **c**, and (**f**) The ROC curves for the propensity model (orange), expected value (green) and weighted propensity (blue).

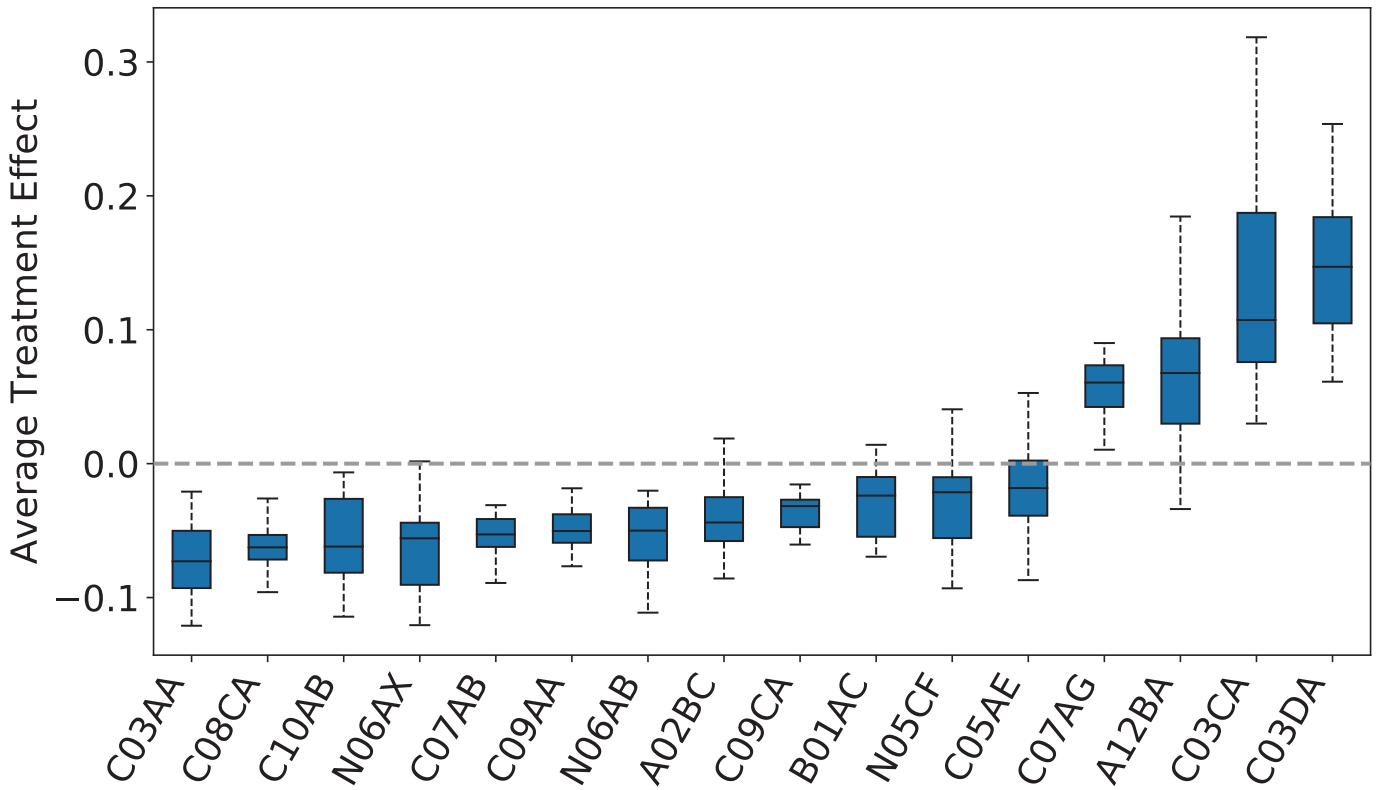

Extended Data Fig. 3 | Distribution of estimated ATE of drug classes on defined outcomes across the 50 bootstrap samples. All these showing drug classes satisfy two conditions: adjusted p-value less than 0.05 and post unbalanced ratio less than 2%. Within the boxplot, the central line denotes the median, and the bottom and the top edges denote the 25th(Q1) and 75th(Q3) and percentiles respectively. The whiskers extend to 1.5 times the interquartile range.

ATC code	Drug class
C03AA	Thiazides, plain
N06AX	Other antidepressants
C08CA	Dihydropyridine derivatives
C10AB	Fibrates
N06AB	Selective serotonin reuptake inhibitors
C07AB	Beta blocking agents, selective
C09AA	ACE inhibitors, plain
A02BC	Proton pump inhibitors
N05CF	Benzodiazepine related drugs
C09CA	Angiotensin II receptor blockers (ARBs), plain
B01AC	Platelet aggregation inhibitors excl. heparin
C05AE	Muscle relaxants
C07AG	Alpha and beta blocking agents
A12BA	Potassium
C03CA	Sulfonamides, plain
C03DA	Aldosterone antagonists

Extended Data Fig. 4 | The list of significant drug classes. The drug classes are denoted using ATC code and corresponding names.

Drug name	# User	# Non-user	Post.unbalanced.ratio%	Pre.ATE	Post.ATE	Adjusted p-value
Metoprolol + Clopidogrel	1237	3711	0.010	-0.034	-0.028	<0.05
Metoprolol + Atorvastatin	2158	6474	0.014	-0.045	-0.024	<0.05
Lisinopril + Atorvastatin	1145	3435	0.015	-0.002	-0.018	<0.05
Carvedilol + Atorvastatin	860	2580	0.011	0.124	0.112	<0.05

Extended Data Fig. 5 | The estimated treatment effects for CAD over balanced and statistically significant drug combinations. The drug combinations are ranked by the estimated ATE values.

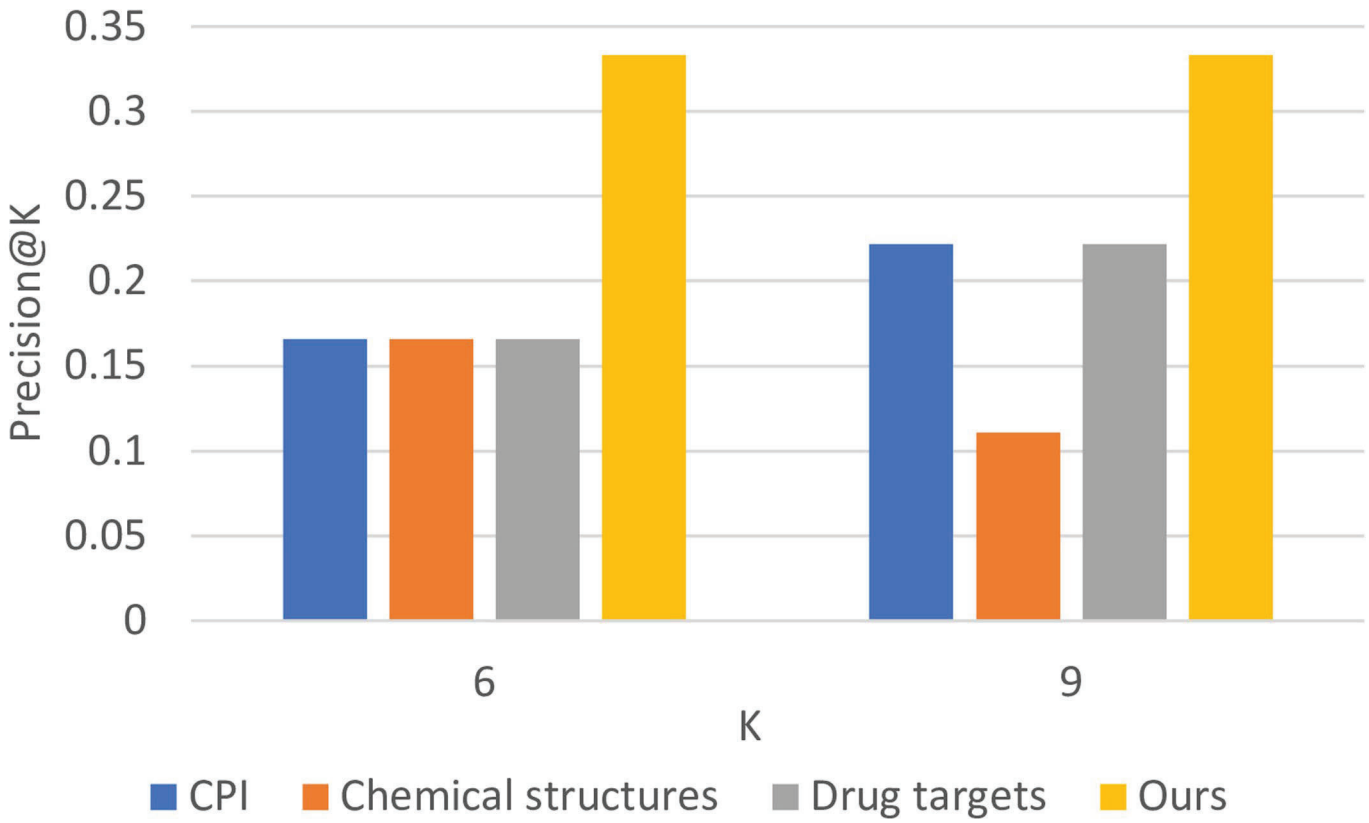

Extended Data Fig. 6 | Performance comparison of proposed method and three pre-clinical methods evaluated by Precision@K. The values of K are selected from {6, 9}.

Threshold (post unbalanced ratio)	Threshold (adjusted p-value)	Drug name	Drug class (ATC code)	Drug class name
<2%	<0.15	Atorvastatin	C10AA	HMG CoA reductase inhibitors
		Metformin	A10BA	Biguanides
		Losartan	C09CA	ACE inhibitors, plain
		Escitalopram	N06AB	Selective serotonin reuptake inhibitors

Extended Data Fig. 7 | Retrieved additional repurposing candidates under different thresholds' setting. The adjusted p-value is changed to 0.15 and the post unbalanced ratio remains the same as previous setting (less than 2%).

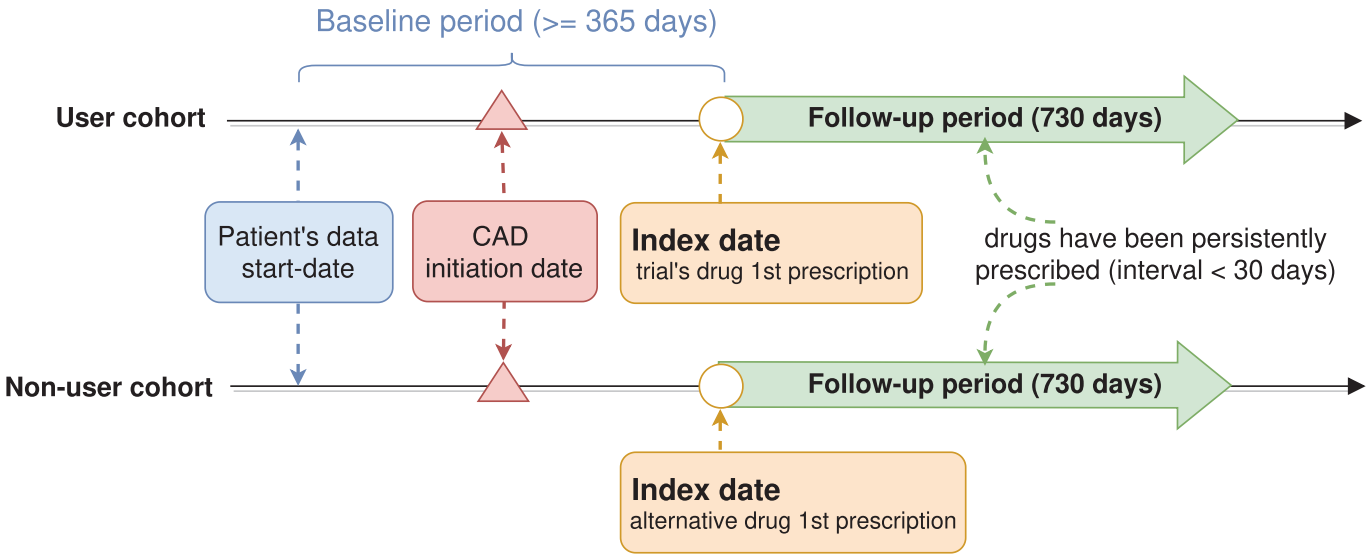

Extended Data Fig. 8 | The definition of user and non-user cohorts. Index date refers to the first prescription of the trial's drug (user cohort) or the alternative drug (non-user cohort). The time period before the index date is the baseline period, and the time after the index date is the follow-up period. The patient covariates are collected during the baseline period and the treatment effects areevaluated at the follow-up period.

nature research

https://doi.org/10.1038/s42256-020-00276-w

Supplementary information

A deep learning framework for drug repurposing via emulating clinical trials on real-world patient data

In the format provided by the authors and unedited

Supplemental Table 1. The definition of coronary artery disease (CAD) from observational health data.

PMID	16159046, 26524702, 28008010
Criteria	• A history of coronary revascularization in the EHR • Or, history of acute coronary syndrome, ischemic heart disease, or exertional angina
Diagnostic codes	**ICD-9 codes:** 410* to 414* **ICD-10 codes:** The best approximation are the following codes: I20* Angina pectoris I21* Acute myocardial infarction I22* Subsequent ST elevation (STEMI) and non-ST elevation (NSTEMI) myocardial infarction I23* Certain current complications following ST elevation (STEMI) and non-ST elevation (NSTEMI) myocardial infarction (within the 28 day period) I24* Other acute ischemic heart diseases I25* Chronic ischemic heart disease

Supplemental Table 2. The definition of heart failure from observational health data.

PMID	26524702, 26687987, 21156884, 15606986
Criteria	Any one of the following: 1. (ICD-9) billing code 2. (ICPC-2-R) diagnosis code 3. "CHF" on the patient's problem list (free text or ICD-9)
Diagnostic codes	**ICD-9 codes:** 402.01, 402.11, 402.91, 428.xx **OR:** 402.01 Hypertensive heart disease, malignant with CHF 402.11 Hypertensive heart disease, benign with CHF 402.91 Hypertensive heart disease, NOS with CHF 404.01 Hypertensive heart/renal disease, malignant with CHF 404.03 Hypertensive heart/renal disease, malignant with CHF + renal failure 404.11 Hypertensive heart/renal disease, benign with CHF 0 (0) 404.13 Hypertensive heart/renal disease, benign with CHF + renal failure 404.91 Hypertensive heart/renal disease, NOS with CHF 404.93 Hypertensive heart/renal disease, NOS with CHF + renal failure 425.xx Cardiomyopathy 428.xx Heart failure **ICD-10 codes:** I11 I13 I50 I42 **ICPC-2-R code:** K77

Supplemental Table 3. The definition of stroke from observational health data.

PMID	29202795
Diagnostic codes	**ICD-9 codes:** V12.54, 438.0–438.9 **ICD 10 codes:** Z86.73 I60-I69 subarachnoid hemorrhage (I60); intracerebral hemorrhage (I61); cerebral infarction (I63); and other transient cerebral ischemic attacks and related syndromes and transient cerebral ischemic attack (unspecified) (G458 and G459),

Supplemental Table 4. Main results for all 55 repurposing drugs.

Drug name	# User	# Non-user	Pre.unbalanced covariates	Post.unbalanced covariates	# Covariates	Post.unbalanced ratio	Pre. ATE	Post. ATE
atorvastatin	13099	39297	16.560	26.200	1300	0.020	-0.029	-0.050
metoprolol	9730	29190	38.308	23.231	1270	0.018	-0.023	-0.043
fenofibrate	1352	4056	39.340	13.200	1038	0.013	-0.051	-0.038
rosuvastatin	2420	7260	24.020	9.620	1097	0.009	-0.063	-0.030
hydrochlorothiazide	2001	6003	32.500	15.320	1076	0.014	-0.055	-0.029
amlodipine	4613	13839	21.340	8.300	1180	0.007	-0.050	-0.026
pravastatin	2007	6021	11.260	9.640	1085	0.009	-0.016	-0.022
simvastatin	1605	4815	10.060	13.240	1044	0.013	-0.032	-0.020
lisinopril	5876	17628	17.960	25.000	1200	0.021	-0.002	-0.020
valsartan	1316	3948	24.940	13.740	1026	0.013	0.010	-0.015
diltiazem	1044	3132	28.360	13.080	1007	0.013	-0.010	-0.013
omeprazole	1916	5748	31.080	15.220	1084	0.014	-0.052	-0.011
losartan	4822	14466	22.680	7.720	1187	0.006	-0.015	-0.007
fluoxetine	505	1515	104.500	46.240	932	0.050	-0.064	-0.005
atenolol	845	2535	42.460	22.460	974	0.023	-0.082	-0.005
metformin	3258	9774	29.700	15.300	1131	0.014	-0.052	-0.004
nebivolol	713	2139	49.960	28.500	958	0.030	-0.083	-0.003
clopidogrel	6488	19464	27.700	7.340	1212	0.006	-0.014	0.013
levothyroxine	2637	7911	39.520	9.380	1131	0.008	-0.034	0.014
escitalopram	1123	3369	56.040	15.460	1025	0.015	-0.036	0.016
gabapentin	1117	3351	74.800	23.220	1041	0.022	0.002	0.016
pantoprazole	2508	7524	21.100	9.780	1114	0.009	0.005	0.019
sertraline	932	2796	60.980	24.140	1013	0.024	-0.036	0.021

benazepril	566	1698	55.120	44.620	907	0.049	-0.068	0.025
bupropion	779	2337	77.920	29.900	979	0.031	-0.050	0.026
aspirin	709	2127	35.260	31.600	952	0.033	-0.010	0.030
isosorbide	1482	4446	33.320	9.560	1039	0.009	0.045	0.034
prasugrel	1316	3948	41.500	18.340	1019	0.018	-0.043	0.036
trazodone	527	1581	128.580	53.440	947	0.057	-0.006	0.039
ramipril	887	2661	25.340	14.840	973	0.015	0.020	0.043
olmesartan	571	1713	73.260	45.400	933	0.049	-0.075	0.047
citalopram	672	2016	56.420	30.440	960	0.032	-0.041	0.060
duloxetine	932	2796	116.300	20.900	1011	0.021	-0.043	0.068
canagliflozin	960	2880	98.900	50.040	993	0.050	-0.053	0.073
potassium chloride	1110	3330	43.460	20.240	1016	0.020	0.169	0.090
ezetimibe	938	2814	67.900	21.220	992	0.021	-0.049	0.090
glipizide	675	2025	63.000	45.240	945	0.048	0.003	0.095
zolpidem	550	1650	88.840	41.940	927	0.045	-0.015	0.106
esomeprazole	446	1338	101.660	57.560	903	0.064	-0.072	0.108
glimepiride	789	2367	70.820	38.380	979	0.039	-0.034	0.112
venlafaxine	606	1818	113.980	58.320	953	0.061	-0.055	0.116
carvedilol	3959	11877	38.280	8.140	1154	0.007	0.198	0.124
ranolazine	587	1761	54.780	42.040	927	0.045	0.036	0.134
sitagliptin	1104	3312	55.400	25.940	1013	0.026	-0.044	0.155
ticagrelor	905	2715	45.360	29.160	979	0.030	-0.002	0.162
furosemide	1545	4635	50.880	17.080	1064	0.016	0.301	0.179
montelukast	908	2724	82.480	27.400	996	0.027	-0.022	0.181
spironolactone	1292	3876	70.620	12.920	1034	0.013	0.393	0.190
allopurinol	865	2595	84.520	26.580	976	0.027	0.025	0.197
alprazolam	492	1476	110.960	49.180	907	0.054	0.006	0.204
oxycodone	575	1725	127.480	50.980	947	0.054	-0.001	0.289
tamsulosin	1137	3411	66.140	27.060	1026	0.026	0.006	0.311
apixaban	710	2130	81.040	41.380	963	0.043	0.168	0.332
rivaroxaban	945	2835	79.080	29.400	1002	0.029	0.102	0.392
warfarin	685	2055	95.760	34.720	952	0.036	0.234	0.540

Supplemental Table 5. Main results for all 38 repurposing drug classes.

Drug name	# User	# Non-user	Pre.unbalanced covariates	Post.unbalanced covariates	# Covariates	Post.unbalanced ratio	Pre. ATE	Post. ATE
A02BA	655	1965	49.450	10.500	557	0.019	-0.025	-0.028
A02BC	3812	10775	19.500	5.300	611	0.009	-0.033	-0.040

A10AE	597	1791	82.150	22.700	545	0.042	0.024	-0.024
A10BA	3252	9756	32.000	14.650	604	0.024	-0.065	-0.086
A10BB	1373	4119	47.700	17.550	575	0.030	-0.016	-0.056
A10BH	1358	4074	57.550	29.850	573	0.052	-0.039	-0.091
A10BJ	735	2205	78.050	24.200	552	0.044	-0.030	-0.051
A10BK	1712	5136	77.700	30.400	584	0.052	-0.039	-0.075
A11CC	543	1629	79.600	13.050	556	0.024	0.030	-0.030
A12BA	1150	3450	40.700	6.500	578	0.011	0.153	0.061
B01AA	677	1596	80.400	22.450	551	0.041	0.197	0.083
B01AC	8451	24429	19.100	4.900	632	0.008	-0.017	-0.030
B01AF	1619	4857	61.200	24.650	586	0.042	0.115	-0.021
C01DA	1535	4605	37.600	4.900	581	0.008	0.053	0.011
C01EB	537	1611	61.600	12.150	532	0.023	0.019	-0.008
C03AA	1989	5967	37.250	9.250	591	0.016	-0.078	-0.075
C03CA	1601	4803	48.200	6.350	588	0.011	0.293	0.128
C03DA	1395	4185	61.150	7.350	577	0.013	0.384	0.151
C05AE	1040	3120	44.150	8.300	569	0.015	-0.011	-0.023
C07AA	657	1971	63.800	11.850	549	0.022	0.053	-0.010
C07AB	10359	28354	16.368	7.000	636	0.011	-0.039	-0.053
C07AG	4040	12120	23.850	4.250	611	0.007	0.187	0.056
C08CA	4801	14403	19.300	5.450	624	0.009	-0.041	-0.063
C09AA	7016	21048	15.650	10.650	629	0.017	-0.007	-0.047
C09CA	5895	17685	14.050	5.200	628	0.008	-0.016	-0.036
C10AA	11730	30838	29.600	15.150	641	0.024	-0.026	-0.064
C10AB	1412	4236	38.350	8.950	572	0.016	-0.047	-0.059
C10AX	979	2937	61.100	12.250	566	0.022	-0.043	-0.049
G04CA	1326	3978	56.800	25.100	580	0.043	-0.019	-0.062
H03AA	2641	7923	42.550	13.200	605	0.022	-0.043	-0.055
M04AA	949	2847	69.550	14.550	558	0.026	0.016	-0.029
N02AA	607	1821	99.800	24.250	553	0.044	-0.040	-0.061
N03AX	1719	5157	69.750	12.450	593	0.021	0.014	-0.032
N05BA	621	1863	86.350	13.400	549	0.024	-0.025	-0.013
N05CF	598	1794	70.500	10.300	550	0.019	-0.026	-0.036
N06AB	2793	8379	41.700	8.300	612	0.014	-0.045	-0.053
N06AX	2279	6837	65.450	11.350	601	0.019	-0.054	-0.066
R03DC	899	2697	65.250	11.300	563	0.020	-0.035	-0.034

Supplemental Table 6. Main results for all 7 repurposing drug combinations.

Drug name	# User	# Non-user	Post unbalanced ratio	Pre.ATE	Post.ATE	Adjusted P-value
Metoprolol + Clopidogrel	1237	3711	0.010	-0.034	-0.028	< 0.05
Metoprolol + Atorvastatin	2158	6474	0.014	-0.045	-0.024	< 0.05
Lisinopril + Atorvastatin	1145	3435	0.015	-0.002	-0.018	< 0.05
Lisinopril + Clopidogrel	630	1890	0.013	-0.018	-0.012	> 0.1
Metoprolol + Lisinopril	962	2886	0.011	-0.028	-0.012	> 0.1
Clopidogrel + Atorvastatin	1477	4431	0.007	-0.019	0.008	> 0.1
Carvedilol + Atorvastatin	860	2580	0.011	0.124	0.112	< 0.05

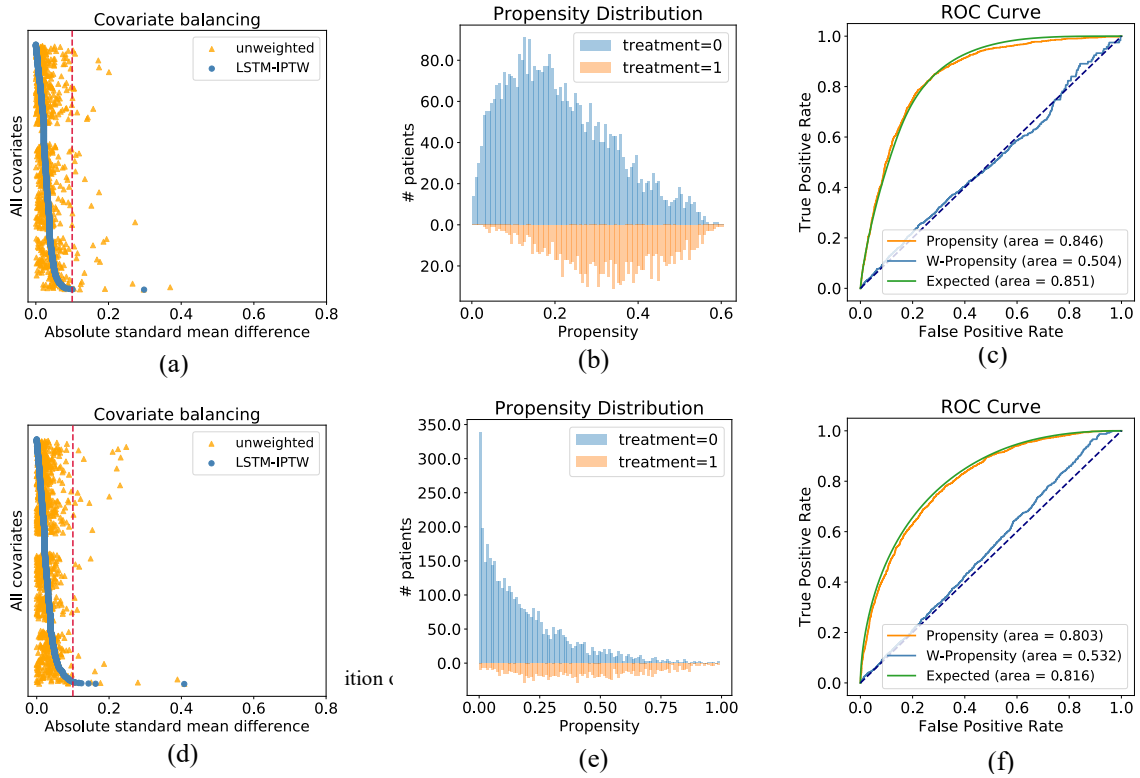

Supplemental Figure 1. Performance comparison of LSTM-IPTW and LR-IPTW on case drug: fenofibrate (*without* known CAD indication). The three figures on the top are results obtained from LSTM-IPTW, and the figures on the bottom are from LR-IPTW. Figure (a) and Figure (d) show the absolute SMD of each covariate in the original data (orange triangles) and in the weighted data (blue circles). Figure (b) and Figure (e) show the distribution of estimated propensity scores over user (orange area) and non-user (blue area) cohorts. Figure (c) and Figure (f) show the ROC curves for the propensity model (orange), expected value (green) and weighted propensity (blue).

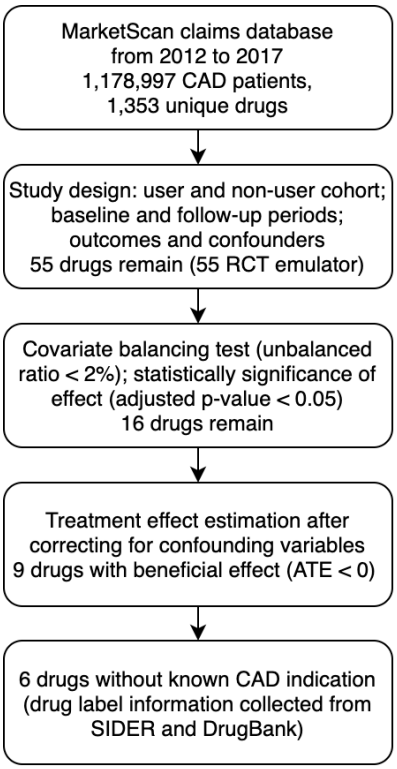

Supplemental Figure 2. Flowchart of data collection and study process of identifying repurposed drug candidates